

Wildfire emissions disrupt black carbon and PM2.5 mortality burden trends across the continental US

Jing Wei^{1,2}, Jun Wang¹, Zhanqing Li², Shobha Kondragunta³, Susan Anenberg⁴, Yi Wang¹, Huanxin Zhang¹, David Diner⁵, Jenny Hand⁶, Alexei Lyapustin⁷, Ralph Kahn⁷, Peter Colarco⁷, Arlindo da Silva⁷, and Charles Ichoku⁸

¹Department of Chemical and Biochemical Engineering, Iowa Technology Institute, Center for Global and Regional Environmental Research, University of Iowa

²Department of Atmospheric and Oceanic Science, Earth System Science Interdisciplinary Center, University of Maryland

³Center for Satellite Applications and Research, NOAA/NESDIS

⁴Department of Environmental and Occupational Health, George Washington University

⁵Jet Propulsion Laboratory, California Institute of Technology

⁶Cooperative Institute for Research in the Atmosphere, Colorado State University

⁷NASA Goddard Space Flight Center

⁸College of Arts & Sciences, Howard University

December 31, 2022

1 **Wildfire emissions disrupt black carbon and PM_{2.5} mortality burden trends**
2 **across the continental US**

3 **Authors:** Jing Wei^{1,2*}, Jun Wang^{1*}, Zhanqing Li², Shobha Kondragunta³, Susan Anenberg⁴, Yi
4 Wang¹, Huanxin Zhang¹, David Diner⁵, Jenny Hand⁶, Alexei Lyapustin⁷, Ralph Kahn⁷, Peter
5 Colarco⁸, Arlindo da Silva⁹, Charles Ichoku¹⁰

6 **Affiliations:**

- 7 1. Department of Chemical and Biochemical Engineering, Iowa Technology Institute, Center for
8 Global and Regional Environmental Research, University of Iowa, Iowa City, IA 52242, USA
- 9 2. Department of Atmospheric and Oceanic Science, Earth System Science Interdisciplinary
10 Center, University of Maryland, College Park, MD 20472, USA
- 11 3. Center for Satellite Applications and Research, NOAA/NESDIS, College Park, MD 20740,
12 USA
- 13 4. Department of Environmental and Occupational Health, George Washington University,
14 Washington, DC 20052, USA
- 15 5. Jet Propulsion Laboratory, California Institute of Technology, Pasadena, CA 91109, USA
- 16 6. Cooperative Institute for Research in the Atmosphere, Colorado State University, Fort Collins,
17 CO 80523, USA
- 18 7. Climate and Radiation Laboratory, NASA Goddard Space Flight Center (GSFC), Greenbelt,
19 MD 20771, USA
- 20 8. Atmospheric Chemistry and Dynamics Laboratory, NASA GSFC, Greenbelt, MD 20771,
21 USA
- 22 9. Global Modeling and Assimilation Office, NASA GSFC, Greenbelt, MD 20771, USA
- 23 10. College of Arts & Sciences, Howard University, Washington, DC 20059, USA

24
25 *Corresponding authors: Jun Wang, jun-wang-1@uiowa.edu ; Jing Wei: jing-wei@uiowa.edu

26 Classification: Physical Science (major), Atmospheric (minor)

27 Keywords: fine particulate matter, black carbon, wildfires, mortality burden, deep learning

30 **Abstract (< 250 words, currently 250)**

31 The long-term improvement trends in air quality and public health in the continental United States
32 (US) were obscured in the past decade by the increase of fire emissions that potentially
33 counterbalanced the decline in anthropogenic emissions. Here, we estimate daily concentrations
34 of fine particulate matter (PM_{2.5}) and its highly toxic component, black carbon (BC), at 1 km
35 resolution in the US from 2000 to 2020 via deep learning that integrates big data from satellites,
36 models, and surface observations. Daily (monthly) PM_{2.5} and BC estimates are reliable with cross-
37 validated R² values of 0.85 (0.98) and 0.79 (0.94), respectively. Both PM_{2.5} and BC in the US show
38 overall decreasing trends of 23% and 18% over the past two decades, leading to a reduction in
39 premature deaths by ~1800 [95% confidence interval (CI): 1300, 2300] people per year. However,
40 the premature death trend has downshifted since 2010; the western US exhibits large interannual
41 fluctuations caused by wildfires, leading to an increase in PM_{2.5} concentrations and associated
42 deaths [~360 (95% CI: [230, 510]) people] per year. In contrast, removing years with large fires
43 would lead to a more significant decreasing trend in PM_{2.5} concentrations. Furthermore, the BC-
44 to-PM_{2.5} mass ratio for the US as a whole shows a significant increase of 1.82% per year, primarily
45 due to the reduction of inorganic emissions and suggesting a potential increase in relative toxicity
46 of PM_{2.5}. Reducing fire risk via effective policies including mitigation of climate warming can
47 substantially improve air quality and public health in the coming decades.

48 **Main text**

49 Atmospheric particulate matter (PM) with an aerodynamic diameter of $\leq 2.5 \mu\text{m}$ (PM_{2.5}) has
50 significant impacts on air quality, climate change, and public health (1, 2). Understanding and
51 estimating these impacts requires knowledge of the spatiotemporal variations of the amount and
52 composition of surface-level PM_{2.5}, but it is challenging due to multiple factors, including the
53 change in and diversity of aerosol sources and aerosol processes as well as the limited number of
54 surface observation sites. Anthropogenic sources are being regulated in many countries, whereas
55 wildfires show significant temporal variations; both are significant contributors to the PM_{2.5} mass
56 and composition, including sulfate, nitrate, ammonium, organic carbon, and black carbon (BC).
57 Of particular importance is BC, due to its strong absorption of solar radiation and consequent
58 warming effect on climate (3, 4) as well as its high toxicity and hence potentially more severe
59 impact on public health (5-9). However, even in the United States (US), where the history records
60 of anthropogenic emissions are well documented, the national outcome of reduced emissions on
61 public health associated with PM_{2.5} and BC exposure still has not been studied on decadal scales
62 (Table S1). Public health outcomes are obscured by large annual fluctuations in fire emissions and
63 associated uncertainties regionally and seasonally. Only a few studies have shown the acute health
64 effects (such as respiratory, cardiovascular, and asthma hospital admissions) from short-term
65 exposure to increased ambient PM_{2.5} and BC mass concentration associated with fire emissions
66 (10-12).

67
68 How have the surface PM_{2.5} mass and its fraction of BC changed in the past two decades in the
69 continental US? And how much change (if any) in mortality burden due to PM_{2.5} exposure may be
70 attributed to fires? Here, we tackle both questions by building upon the advances enabled by
71 machine learning (ML) and the long-term data record of aerosol measurements from both space
72 and the surface over the US. Past studies have integrated satellite-based aerosol optical depth
73 (AOD) products together with in situ ground measurements to estimate surface PM_{2.5} over the US
74 via approaches such as kriging (13), land-use regression modeling (14), neural network (15),
75 random forest (16), geographically weighted regression (17), ML ensemble-based modeling (18),
76 and convolutional neural network (19). Unlike PM_{2.5}, there are few studies focusing on BC
77 estimates in the US (9, 17). The time periods of most previous studies are particularly short (< 10
78 years, Table S1). Although it has been postulated that the PM_{2.5} concentration in the US should be

79 declining due to persistent regulations to reduce anthropogenic emissions since enactment of the
80 Clean Air Act (CAA) of the 1970s, this conjecture cannot be fully verified with surface observation
81 alone because it lacks full continental spatial coverage, especially when considering the recent
82 increase of fires in the western US (20-23). As fire emissions are the second-largest source of BC
83 in the US and a key source of PM_{2.5} in fire-prone areas (24, 25), both the amount and the toxicity
84 of ambient PM_{2.5} could be increased, which leads to the hypothesis that the overall PM_{2.5} impact
85 on the public health burden may not change at all or might even have increased in the US in the
86 past two decades, at least in the west.

87
88 We derived surface PM_{2.5} and BC concentrations from 2000 to 2020 in the US with full spatial
89 coverage via the deep learning (DL) approach and estimated the mortality burden in terms of the
90 number of premature deaths associated with the change of PM_{2.5} and BC at the national and
91 regional scales. Our DL-based method integrates multiple sources of satellite-based data products,
92 reanalysis datasets of aerosol composition, and datasets from surface monitoring stations in the
93 US. Our method mitigates the impacts of the missing data associated with the spatial gaps in the
94 satellite AOD retrievals due to clouds and surface snow or ice cover, and considers both spatial
95 and temporal variations of the AOD-PM_{2.5} relationship. Our long-term estimate of BC is made
96 daily at 1 km resolution, in contrast with past studies that used chemical transport models at a
97 much coarser resolution (50 km or larger) (9) and monthly or annual averages (17) (Table S1).

98
99 The association of health outcomes with exposure to PM_{2.5} is often assessed by integrating PM_{2.5}
100 mass concentration and population density distribution with different concentration-response
101 functions (CRFs), such as the Integrated Exposure–Response (IER) model (26). The IER model
102 was defined by the Global Burden of Disease (GBD) 2017 study (27) and was further updated in
103 the recent GBD 2019 study (28). Using the IER model, Apte et al. (29) illustrated that the emission
104 reduction of global PM_{2.5} to meet the World Health Organization guidance could have avoided 23%
105 of the population deaths attributable to ambient PM_{2.5} in 2010. However, the CRFs in the IER
106 model are steeper in clean areas, suggesting higher sensitivity of the mortality burden to the change
107 of PM_{2.5} by fire emissions in the US than in more polluted countries (such as China or India). Wang
108 et al. (30) found that, in California, the mortality burden in 2012 from exposure to air pollution
109 that originated in nonlocal sources was greater than that caused by local anthropogenic emissions.

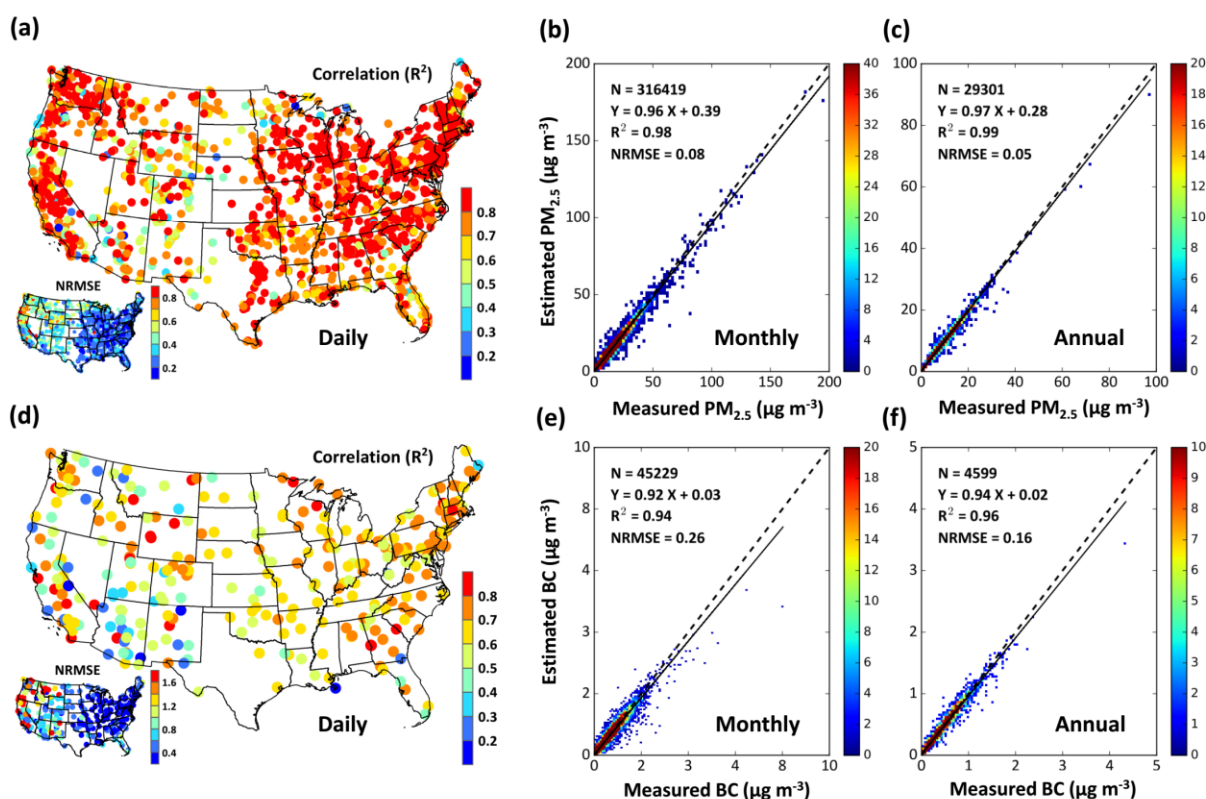
110 Aguilera et al. (31) found that the PM_{2.5} generated from the wildfires had larger effects on the
111 human respiratory system than PM_{2.5} from other sources in Southern California during 1999–2012.

112
113 Although the mortality burden associated with PM_{2.5} exposure has been estimated in many studies,
114 few have investigated the health impacts of BC in the US (7-9, 32), which is due in part to the
115 limited availability of both exposure data sources and CRF for BC. Smith et al. (32) calculated the
116 mortality effects related to long-term BC exposure in 66 US cities through the cohort study. Pond
117 et al. (7) and Wang et al. (8) documented two cohort studies showing the significant positive
118 associations of cardiopulmonary and all-cause mortality, respectively, with exposure to major
119 PM_{2.5} components, especially BC, in the US. Li et al. (9) estimated ~14,000 premature deaths
120 caused by ambient BC in 2010 in the US. Here, we study the long-term (2000–2020) mortality
121 burden from exposure to both PM_{2.5} and its BC component at each 1 km² grid in the continental
122 US and investigate the role of fire emissions in changing the annual mortality burden since the
123 start of the new millennium. For the mortality burden assessment, the CRF of PM_{2.5} was collected
124 from GBD 2019, and a sensitivity study was also conducted by taking the CRF of BC from the
125 literature to consider the potentially greater toxicity of BC compared with other PM_{2.5} components
126 (see Materials and Methods).

127 128 **Results and Discussion**

129 **Evaluation of PM_{2.5} and BC predictions.** The daily PM_{2.5} and BC estimates at 1 km resolution
130 in the continental US are evaluated via the widely used 10-fold cross-validation approach (33, 34).
131 The DL-based approach works well in capturing daily surface PM_{2.5} levels. At more than 82% and
132 79% of surface observation sites, cross-validation yields high R² (coefficient of determination)
133 values greater than 0.7, and low values of normalized root mean square error (NRMSE) less than
134 0.4, respectively, especially for the eastern US (Fig. 1a). With a spatial distribution pattern similar
135 to that of surface PM_{2.5}, surface BC estimates overall have slightly smaller R² values compared to
136 ground-based observations (Fig. 1d), indicating a relatively decreasing accuracy in our estimates
137 due to the much smaller concentration of BC and the relatively large uncertainty of BC
138 measurements (a factor of two as compared to 10% for PM_{2.5}) (35, 36). For the 21-year study
139 period in the US, all daily PM_{2.5} and BC estimates show high fidelity, with average R² values of
140 0.85 and 0.79 against surface observations, and exhibit NRMSE values of 0.33 and 0.61,

141 respectively (Fig. 1a and 1d). These statistical agreements are further improved upon in the
 142 comparisons of monthly (i.e., $CV-R^2 = 0.98$ and 0.94 , $NRMSE = 0.08$ and 0.26 , Fig. 1b and 1e)
 143 and annual (i.e., $CV-R^2 = 0.99$ and 0.96 , $NRMSE = 0.05$ and 0.16 , Fig. 1c and 1f) averages. In
 144 addition, in terms of overall accuracy, our $PM_{2.5}$ and BC estimates are more reliable than or
 145 comparable to those in previous studies with reference to ground measurements on different
 146 temporal scales (Table S1) (14-19), which ensures that the exposure data of $PM_{2.5}$ and BC have
 147 the accuracy needed for assessing the effects of long-term $PM_{2.5}$ exposure on public health.
 148



149
 150 **Fig. 1.** Spatial distribution of R^2 in the cross-validation of daily (a) $PM_{2.5}$ and (d) BC estimates
 151 (unit: $\mu g m^{-3}$) at each ground monitoring station during the years 2000–2020 in the US. Also
 152 shown are the inter-comparison of measured (x-axis) and estimated (y-axis) of (b & e) monthly
 153 and (c & f) annual $PM_{2.5}$ (top row) and BC concentration (bottom row), respectively, in units of
 154 $\mu g m^{-3}$. The insets in (a) and (d) show the spatial distribution of normalized root mean square
 155 error (NRMSE).
 156

157 **Spatiotemporal variations of $PM_{2.5}$, BC, and mortality burden.** Figure 2 shows the
 158 spatiotemporal distribution on average and the trend of $PM_{2.5}$, BC, and mortality burden in the US
 159 during the years 2000–2020 (maps for each year are provided in the Supplementary Information

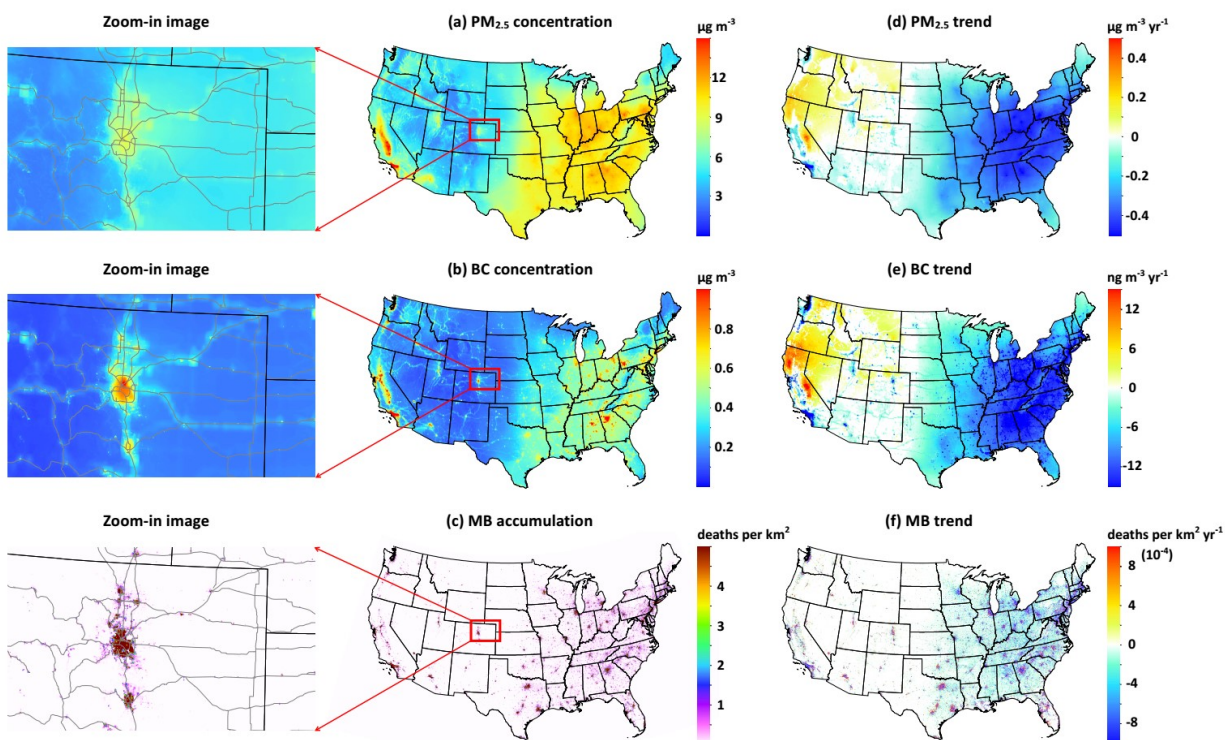
160 (SI) in Figs. S1-S3). Both annual PM_{2.5} and BC concentrations have similar spatial distributions;
161 their mean values of $9.5 \pm 2.0 \mu\text{g m}^{-3}$ and $0.44 \pm 0.16 \mu\text{g m}^{-3}$ in the eastern US (EUS) are about
162 1.9 and 2.2 times higher than their counterparts in the western US except California (WUS, Fig.
163 2a, b) and 1.2 and 1.5 times higher than those in the central US (CUS), which reflects the
164 population distribution and anthropogenic emissions. At the individual state level, the highest
165 persistent pollution levels are found in some areas in California, likely reflecting the wildfire
166 smoke patterns and local source of dust, especially in the central valley. Indeed, both PM_{2.5} and
167 BC increase by 35–38% in the fire seasons (autumn and summer) when compared to normal
168 seasons (spring and winter) in the WUS (Figs. S4-S5). The cumulative number of premature deaths
169 associated with exposure to PM_{2.5} pollution in most parts of the US is relatively small because of
170 the small population density in these areas. The total mortality burden in the continental US is
171 estimated to be ~1.8 million (95% CI: [1.1, 2.6]) during the 21-year period of this study (Fig. 2c).
172 As expected, these premature deaths were mainly concentrated in cities with large populations,
173 such as Los Angeles, Houston, Chicago, Atlanta, and New York. In addition, our 1 km high-
174 spatial-resolution data allows us to study air pollution and its impacts on public health at a much
175 finer scale (see magnified images in Fig. 2). Large differences in the pollution levels of urban and
176 rural regions can be clearly seen; in particular, high BC concentrations along highways due to
177 traffic-related emissions (from diesel trucks) are well captured. In addition, contrasting
178 distributions in the mortality burden in large cities and their surrounding areas can also be well
179 characterized. These results highlight the unique advantages of high-resolution air pollution data.

180

181 Temporally, the annual amounts of PM_{2.5} and BC in the years 2000–2020 show steadily declining
182 trends in the EUS, remain nearly the same in the CUS (Fig. 2d-e), and fluctuate with large
183 variations in sign and magnitude across the WUS. In the WUS, significant decreasing trends were
184 observed in the city clusters located in the southwest (Los Angeles) and northwest (Seattle) corners;
185 by contrast, significant increasing trends were found in most central inter-mountainous and
186 northwest areas, especially Northern California and Oregon. At the seasonal scale, declining trends
187 throughout the US were found in winter and spring; however, in summer and autumn, trends were
188 opposite, increasing in the WUS and decreasing in the EUS (Fig. S6-S7), which suggests the
189 increasing impacts of wildfires on surface PM_{2.5} and BC, as these are the fire seasons in the WUS
190 (37, 38). Overall, in the past two decades, the total number of premature deaths associated with

191 exposure to PM_{2.5} has reduced ($> 10^{-3}$ per km² per year) in populated parts of the US, especially
 192 in the EUS. It is also worthy to mention that this was also observed in places where PM_{2.5} pollution
 193 go down, but population go up (Fig. S8), which was mainly contributed to the improved air quality.
 194 Regionally, an increased number of deaths is found only in a few large cities located in the western
 195 and southern US (Fig. 2f), which may be attributed to an increase in local fire and dust emissions
 196 (20, 23, 39), transboundary transport from Mexico (40, 41), and/or an increase in population
 197 density (Fig. S8).

198



199

200 **Fig. 2.** Spatial distribution of the annual mean (a) PM_{2.5} concentration (unit: $\mu\text{g m}^{-3}$), (b) BC
 201 concentration (unit: $\mu\text{g m}^{-3}$), (c) total cumulative mortality burden (MB) (unit: premature deaths
 202 per km²) during the years 2000-2020 in the US, and zoomed-in images (left column) for the Denver
 203 area, in which the gray lines represent the roads, and (d-f) represent corresponding annual trends
 204 across the US. Only the trends that are significant at the 95% ($p < 0.05$) confidence level are shown.
 205

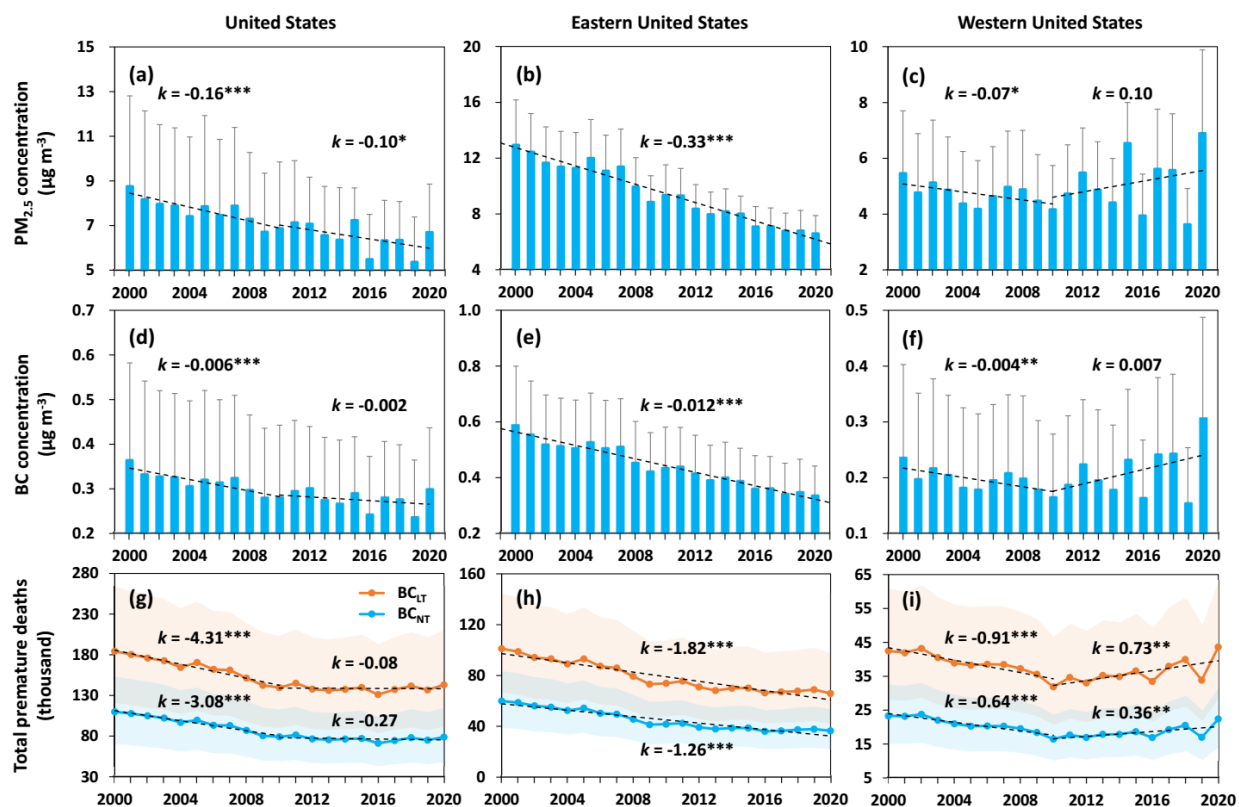
206 The trends of the time series of annual mean PM_{2.5}, BC, and premature deaths during the years
 207 2000–2020 were analyzed for the continental US, EUS, and WUS (Fig. 3). At the national level,
 208 PM_{2.5} and BC concentrations overall declined by $\sim 23\%$ and 18% during the entire period, with the
 209 highest and lowest levels in 2000 and 2019, respectively. The decreasing trends were larger in the

210 first decade and slowed in the second decade (Fig. 3a, d). Looking geographically, greater
211 declining trends of 49% and 43% with small fluctuations were seen in the EUS (42) (Fig. 3b, e),
212 whereas in the WUS, virtually no trends existed during the entire period due to larger interannual
213 fluctuations (Fig. 3c, f), particularly in summer and autumn (Fig. S9c, f). More importantly,
214 significant downward trends ($p < 0.1$ and 0.05) were observed before 2010 but were then reversed
215 (slope > 0), likely showing the impact of increasing fire emissions in recent years (as revealed in
216 the analysis below).

217

218 The annual number of total premature deaths exposure to PM_{2.5} pollution across the continental
219 US first significantly decreased from 110 [95% confidence interval (CI): 71, 154] thousand in
220 2000 to 79 (95% CI: 50, 114) thousand in 2010; it then stabilized at nearly constant level with only
221 small fluctuations (blue line in Fig. 3g). A continuous decrease in deaths at a significant rate of
222 ~1260 people per year ($p < 0.01$) was observed in the EUS (blue line in Fig. 3h). In contrast, in the
223 WUS (blue line in Fig. 3i), the annual death burden had a steady decrease (slope = -0.64 thousand
224 per year, $p < 0.01$) until 2010 [16 thousand; 95% CI: (10, 24)], after which there was a significant
225 increase (slope = 0.36 thousand per year, $p < 0.05$) with large annual fluctuations, leading to the
226 peak burden in 2020 [22 thousand; 95% CI: (14, 32)].

227



228
 229 **Fig. 3.** Time series of annual and area mean of (a-c) $\text{PM}_{2.5}$ concentrations ($\mu\text{g m}^{-3}$), (d-f) BC
 230 concentrations ($\mu\text{g m}^{-3}$), and (g-i) total premature deaths (unit: thousand) associated with the total
 231 $\text{PM}_{2.5}$ pollution in the years 2000–2020 in the continental US, eastern US, and western US,
 232 respectively. Orange and blue lines denote the estimates of premature deaths with and without
 233 considering the larger toxicity of BC (BC_{LT} and BC_{NT}), respectively. The regression lines are
 234 shown as black dotted lines, and their slope (k) values are also given with *, **, and ***,
 235 representing trends that are significant at the 90% ($p < 0.1$), 95% ($p < 0.05$), and 99% ($p < 0.01$)
 236 confidence levels, respectively.

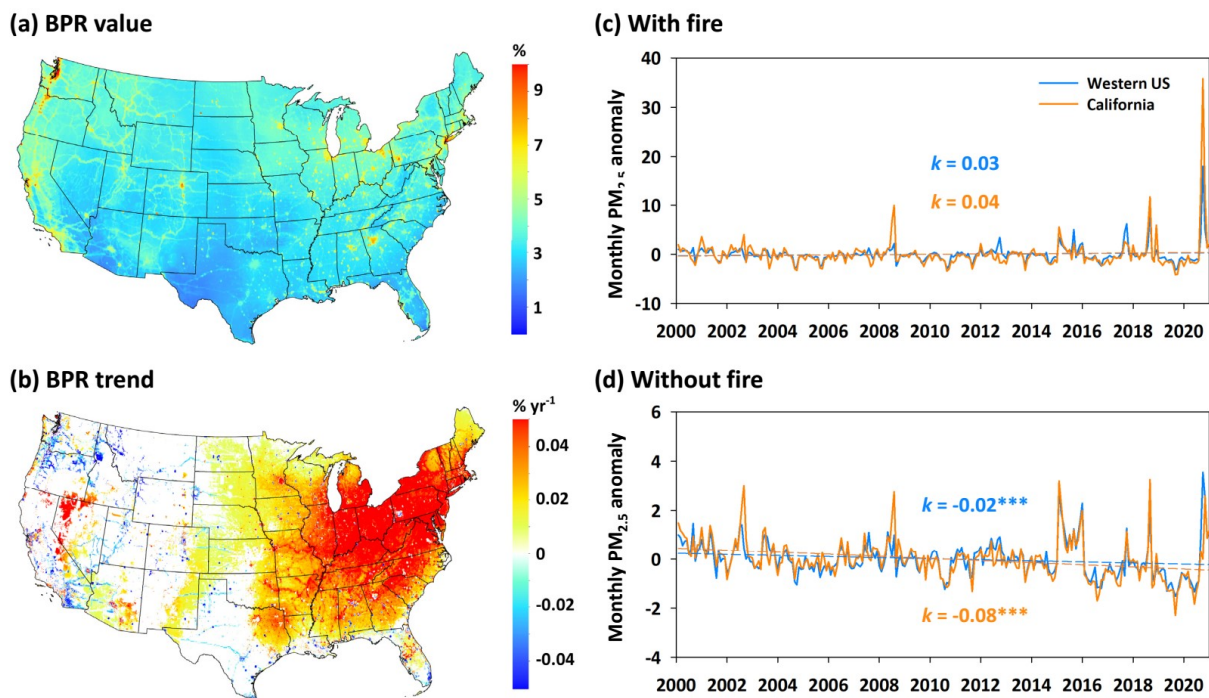
237
 238 **Impact of fire emissions and importance of BC on premature mortality.** As more recent cohort
 239 studies have documented the importance of aerosol composition, especially BC, for the assessment
 240 of mortality burden, it is necessary to analyze not only the absolute amount but also the fractional
 241 concentration of BC. Figure 4 shows the spatiotemporal variations of BC-to- $\text{PM}_{2.5}$ ratio (BPR) in
 242 summer from 2000 to 2020. High BPR values of 5-10% are mainly distributed in major
 243 metropolitan areas (Seattle, San Francisco, Denver, etc.), consistent with the mass fraction of BC
 244 in anthropogenic emissions of $\text{PM}_{2.5}$ (24). Although it varies, the BC mass fraction in fire
 245 emissions of $\text{PM}_{2.5}$ is generally less than 5% (43). Therefore, no significant trend of BPR can be
 246 found in fire-prone areas in the WUS, except in rural and remote areas where an increasing trend
 247 exists, likely due to either local wildfire emissions or the transport of smoke particles from the

248 upwind region (Fig. 4b). In addition, no significant trend in BPR values is found in the southern
249 parts of the Gulf states in the US (Fig. 4b), which may be a result of fire emissions from prescribed
250 burns (44). Overall, however, BPR values increased throughout the US with an average value of
251 1.82% per year ($p < 0.01$), primarily driven by the increase in the EUS, reflecting a faster decline
252 of other PM_{2.5} components such as sulfate and nitrate concentration as a result of the large
253 reduction in emissions of nitrogen and sulfur oxides dioxide (45-47).

254

255 In the WUS, especially in rural areas of California, Nevada, Arizona, and New Mexico, the
256 significant increase in BPR can be explained by the high consistency between the annual mean
257 PM_{2.5} and BC concentrations ($p < 0.01$) and the high correlation of BPR changes with the fire
258 emissions of smoke particles during the last two decades, at a statistically significant level ($p <$
259 0.1) since 2010 (Fig. S10). Indeed, in the WUS and California, the time series of monthly PM_{2.5}
260 anomaly shows large fluctuations in some individual years associated with large fires, e.g., 2020,
261 2017, and 2018 (Fig. 4c), when PM_{2.5} concentrations are much higher, with estimates of 46%, 31%,
262 and 30% from wildfires in the WUS, respectively. After these years of heavy wildfire events are
263 removed, the original overall upward trend of PM_{2.5} is replaced by an opposite significant
264 downward trend ($p < 0.01$) of PM_{2.5} pollution in the WUS, especially in California ($p < 0.01$) (Fig.
265 4d). This attests to the importance of the combined effects of fire emissions and the long-term
266 reduction of anthropogenic emissions in regulating the ambient PM_{2.5} concentration.

267



268
 269 **Fig. 4.** Spatial distribution of (a) mean (unit: %) and (b) trends (unit: % yr⁻¹) of BC-to-PM_{2.5} ratios
 270 (BPR) in summer during the period 2000–2020 across the continental US. Also shown are the time
 271 series of monthly PM_{2.5} anomalies (c) before and (d) after removing the years of wildfires from
 272 2000 to 2020 in the western US (blue lines) and California (orange lines), respectively. In (b), only
 273 the trends that are significant at the 95% ($p < 0.05$) confidence level are shown. In (c-d), the
 274 regression lines are colored by region, and their slope (k , units: $\mu\text{g m}^{-3} \text{ yr}^{-1}$) values are given with
 275 *, **, and ***, representing trends that are significant at the 90% ($p < 0.1$), 95% ($p < 0.05$), and
 276 99% ($p < 0.01$) confidence levels, respectively.
 277

278 The toxicity of BC to human health remains uncertain in the literature. Many studies illustrate that
 279 BC has a larger relative risk and, therefore, a larger impact on mortality than other PM_{2.5}
 280 components (5-8), but some others suggest low confidence (48). As a sensitivity study, we
 281 compared estimates of premature deaths under the assumption that BC is no more toxic than and
 282 has a similar impact on health as non-BC PM_{2.5} constituents (blue lines in Fig. 3g-i) with deaths
 283 calculated assuming larger BC toxicity (orange lines in Fig. 3g-i). We found that the mortality
 284 burdens of total PM_{2.5} could be increased by 80-100% and that their trends could have accelerated
 285 much more in recent years. This acceleration was distinct in the WUS (slope = 0.73 thousand or
 286 730 per year, $p < 0.05$), resulting in extra loss of life (due to higher toxicity) at the increasing rate
 287 of 370 people per year (Fig. 3i), suggesting that the mortality burden is highly related to the
 288 variations of BC and that the increasing number and intensity of wildfires in recent years led to

289 the reversal of the otherwise decreasing trend. Hence, this sensitivity analysis highlights the
290 importance of future studies to accurately define the CRF for BC.

291

292 **Summary and Conclusion**

293 By combining the long-time-series and high-quality observations of the amounts and compositions
294 of surface PM_{2.5} mass in the US with satellite observations and model reanalysis, we developed a
295 deep-learning approach to generate daily 1-km-resolution, high-quality PM_{2.5} concentrations with
296 full spatial coverage for 21 years (2000–2020) and derived the BC component (often found to be
297 more strongly associated with premature mortality than other aerosol components). The nation-
298 wide PM_{2.5} and BC products estimated in this study agree well with ground-based measurements
299 at highly limited stations. Based on the uniform and fine-resolution data sets, we further
300 investigated the long-term trends of both PM_{2.5} and BC pollution in the US during the last two
301 decades and assessed their impacts on mortality burden at a 1 km fine grid. While PM_{2.5} and BC
302 concentrations have decreased considerably and the mortality burden associated with PM_{2.5}
303 pollution was alleviated overall in 2000–2020 in the continental US, the BC concentration declined
304 at a slower pace and non-uniformly with time. As a result, PM_{2.5} could be relatively more toxic
305 due to the increase of BPR in the US. Furthermore, fire emissions in recent years have led to a
306 national slowdown and a regional reversal in the WUS of the declining trend of mortality burden
307 associated with PM_{2.5} and BC, not only during fire seasons but also at the annual scale. Sensitivity
308 studies underscored the importance of future work to further examine the concentration-response
309 function to BC, especially during fire seasons. The potentially larger toxicity of BC compared to
310 other PM_{2.5} components could further exacerbate the health outcomes associated with the
311 slowdown in the decrease of PM_{2.5} concentration due to fires. The policies to mitigate climate
312 change have co-benefits of reducing not only the impact of heatwaves but also the impact of fire
313 emissions and aerosol composition, especially BC, on public health (49).

314

315 **Materials and Methods**

316 **Big Data.** Measurements of surface 24-hour-average PM_{2.5} and BC concentrations were collected
317 daily from the Environmental Protection Agency (EPA) Air Quality System (AQS) and Chemical
318 Speciation Monitoring Network (CSN) and every third day from the Interagency Monitoring of
319 Protected Visual Environments (IMPROVE) (50, 51) at approximately 2740 monitoring stations

320 from 2000 to 2020 throughout the US. Spatial representation has been improved by integrating the
321 EPA and IMPROVE networks, in which monitors are distributed mainly in urban and rural areas,
322 respectively.

323
324 Daily 1-km-resolution Multi-Angle Implementation of Atmospheric Correction (MAIAC)
325 Collection 6 AOD (at 550 nm) products (MCD19A2) retrieved from Moderate Resolution Imaging
326 Spectroradiometer (MODIS) instruments on Terra (~10:30 a.m. local time) and Aqua (~1:30 p.m.
327 local time) satellites since their respective inception (February 25, 2000, and July 4, 2002) to the
328 end of 2020 were employed (52). Also used in the estimates of the surface BC was the Multi-angle
329 Imaging SpectroRadiometer (MISR) Version 23 Level 3 monthly absorbing AOD product (~0.5
330 degrees) (53). Total aerosol extinction AOD, absorbing AOD (calculated by subtracting scattering
331 AOD from total AOD), black carbon extinction AOD, and the surface mass concentrations of
332 different aerosol components, including BC, organic carbon, dust, sulfate, and sea salt) were
333 collected from MERRA-2 aerosol diagnostics at a horizontal resolution of $0.625^\circ \times 0.5^\circ$ (54).
334 Monthly anthropogenic emissions, including BC, nitrogen oxides, ammonia, sulfur dioxide, and
335 volatile organic compounds, were obtained from the Copernicus Atmosphere Monitoring Service
336 (CAMS) global emission inventories (~0.1 degrees) (55). In addition, monthly smoke emissions
337 from the Fire Energetics and Emissions Research (FEER) database (~0.5 degrees before 2003 and
338 0.1 degrees after 2003) (56).

339
340 Meteorological fields were extracted from ERA5 global reanalysis (~0.1°–0.25° degrees) (57, 58),
341 including the 2 m temperature, precipitation, evaporation, relative humidity, 10 m u-component
342 and v-component of winds, surface pressure, boundary layer height, and surface solar radiation
343 downwards. In addition, the 90 m Shuttle Radar Topography Mission (SRTM) digital elevation
344 model (59), monthly 1 km MODIS normalized difference vegetation index (60) and annual 1 km
345 LandScanTM global population distribution (61) products were also used as inputs in machine
346 learning and prediction. All the auxiliary variables above were aggregated or resampled (using the
347 bidirectional linear interpolation approach) to $0.01^\circ \times 0.01^\circ$ grids (≈ 1 km) to be compatible with
348 the resolution of MAIAC AOD products.

349

350 **Surface PM_{2.5} and BC estimates with deep learning.** A deep learning model was trained by
351 using the aforementioned satellite data and model outputs as features and surface measurements
352 of PM_{2.5} and BC as targets. MAIAC AOD was the primary input to the deep-learning model for
353 PM_{2.5} estimation. Terra and Aqua MODIS AOD values were first integrated using a linear
354 regression model to minimize the difference caused by different observation times and enlarge the
355 spatial coverage (62). In conditions of clouds and snow/ice surfaces and places with satellite swath
356 gaps where MAIAC AOD was missing, AOD values were provided by using MERRA-2 reanalysis.
357 MERRA2 AOD data is generated by assimilating a variety of satellite retrievals (including MODIS)
358 and ground-based observations and has been shown to have accuracy comparable to satellite AOD
359 data in areas with high-density observation networks (e.g., North America and Europe) (63, 64).

360

361 To improve the estimates of PM_{2.5}, the spatiotemporal autocorrelation and difference in PM_{2.5} were
362 considered in the deep learning, i.e., deep forest (DF) (65), leading to a novel spatiotemporal
363 weighted deep forest (SWDF) model (for details, see SI Text S1). Deep forest is a deep learning
364 model that uses the Cascade structure by including multiple random forests and extremely
365 randomized trees in each middle layer. The final result was determined by integrating the results
366 of all intermediate hidden layers using the Light Gradient Boosting Machine.

367

368 Specifically, the model construction included two main steps: we first derived daily PM_{2.5} by
369 training the SWDF model between PM_{2.5} measurements and AOD together with PM_{2.5} components,
370 meteorological fields, anthropogenic emissions of PM_{2.5} precursors, and land-use and population
371 variables. Once PM_{2.5} estimates were made, they were subsequently used as the main predictor in
372 the SWDF model to predict BC mass concentration; additional factors highly associated with BC,
373 e.g., the absorbing AOD and BC AOD, and BC surface mass concentrations and emissions, were
374 also used as inputs in training (for details, see SI Text S1).

375

376 For model training, since there were enough data samples for PM_{2.5} every year (i.e., the number of
377 samples, N , ranges from 160,000 to 370,000 per year; total N of all years = 5,931,081), data
378 collected each year from 2000 to 2020 were used to train the SWDF model for that year. Differing
379 from PM_{2.5}, all data samples of BC ($N = 467,002$) collected from the years 2000–2020 were used

380 together to construct the SWDF model for all years since the number of surface BC monitors is
381 smaller than that of PM_{2.5} throughout the US.

382

383 **Mortality Burden Assessment.** The total premature deaths from exposure to ambient PM_{2.5}
384 pollution was calculated at each grid box of 1 km in the US for each year from 2000 to 2020 using
385 the concentration-response functions from the GBD 2019 study (28). The GBD framework
386 integrates relative risk with population density, the number of people in each age group, and
387 baseline cause-specific mortality to estimate cases of cause-specific mortality that are attributable
388 to PM_{2.5} (Equation 1). This calculation was carried out separately for mortality from six diseases
389 (i.e., acute lower respiratory infection, chronic obstructive pulmonary disease, ischemic heart
390 disease, lung cancer, stroke (ischemic and hemorrhagic), and diabetes (Type 2)) at 16 different age
391 groups (i.e., children < 5 years old; adults 25-95 at intervals of 5, and > 95 years old), which are
392 then summed to yield total PM_{2.5}-attributable mortality:

393
$$MB_{PM_{2.5}(d,a,y)} = \frac{RR_{d,a,y-1}}{RR_{d,a,y}} \times B_{d,a,y} \times P_y \quad (1)$$

394 where $MB_{PM_{2.5}(d,a,y)}$ indicates the mortality burden from the exposure to ambient PM_{2.5}, i.e., the
395 number of premature deaths caused by disease d for age group a in year y , and $RR_{d,a,y}$ and $B_{d,a,y}$
396 are the relative risk and baseline mortality of disease d for age group a in year y , which are collected
397 from the disease- and age-specific risk look-up table exceeding the theoretical minimum risk
398 exposure level (TMREL: 2.4–5.9 $\mu\text{g m}^{-3}$) and from the mortality rate data provided by the GBD
399 2019, respectively. P_y indicates the population in age group a in year y , where the population data
400 is collected from the LandScanTM global population database at a 1 km resolution.

401

402 The mortality risk of BC to public health is reported to be more harmful (up to ten times higher)
403 than PM_{2.5} (5-8), but no universal concentration-response function for BC is available. Thus, the
404 health burden of BC is assessed by employing the pooled estimate of concentration-response
405 function exposure to long-term BC pollution, i.e., the relative risk per 1 $\mu\text{g m}^{-3}$ increase in BC for
406 all-cause mortality is 1.06 (95% CI: 1.04, 1.09) (5).

407

408 **Acknowledgments.** This work is supported in part by the NASA Applied Science program (grant
409 numbers: 80NSSC19K0191, 80NSSC21K0428, and 80NSSC21K1980) and NASA's MAIA

410 satellite mission (managed by JPL with contract number 1583456 to the University of Iowa), as
411 well as NOAA's GEO-XO project (grant #: NA21OAR4310249 and NA21OAR4310250) and the
412 NOAA Atmospheric Chemistry, Carbon Cycle and Climate (AC4) program (NA19OAR4310178).
413 C.I. acknowledges support from the NOAA Educational Partnership Program with Minority
414 Serving Institutions (NOAA/EPP/MSI under agreement no. NA16SEC4810006). J.W. also thanks
415 Dr. Jeffrey S. Reid for useful exchanges on fire emission factors of black carbon. The contributions
416 of D.J.D. are carried out at the Jet Propulsion Laboratory, California Institute of Technology, under
417 contract with NASA. The scientific results and conclusions, as well as any views or opinions
418 expressed herein, are those of the author(s) and do not necessarily reflect those of NOAA or the
419 Department of Commerce.

420
421 **Data availability.** All study data are included in the article and/or SI Appendix. The generated 1-
422 km-resolution PM_{2.5} and BC data of this study are available from the corresponding authors upon
423 request and will be made publicly available once the paper is published. Previously published data
424 were used for this work, and the links for each dataset can be found in the SI Appendix (see SI
425 Text S2).

426

427 **References**

- 428 1. Ramanathan V & Feng Y (2009) Air pollution, greenhouse gases and climate change:
429 Global and regional perspectives. *Atmos Environ* 43(1):37-50.
- 430 2. Hong CP, *et al.* (2019) Impacts of climate change on future air quality and human health
431 in China. *P Natl Acad Sci USA* 116(35):17193-17200.
- 432 3. Bond TC, *et al.* (2013) Bounding the role of black carbon in the climate system: A scientific
433 assessment. *J Geophys Res-Atmos* 118(11):5380-5552.
- 434 4. Ramanathan V & Carmichael G (2008) Global and regional climate changes due to black
435 carbon. *Nat Geosci* 1(4):221-227.
- 436 5. Janssen NAH, *et al.* (2011) Black Carbon as an Additional Indicator of the Adverse Health
437 Effects of Airborne Particles Compared with PM₁₀ and PM_{2.5}.
438 119(12):1691-1699.
- 439 6. Yang Y, *et al.* (2019) Short-term and long-term exposures to fine particulate matter
440 constituents and health: A systematic review and meta-analysis. *Environ Pollut* 247:874-
441 882.
- 442 7. Pond ZA, *et al.* (2021) Cardiopulmonary Mortality and Fine Particulate Air Pollution by
443 Species and Source in a National U.S. Cohort. *Environmental Science & Technology*.
- 444 8. Wang Y, *et al.* (2022) Long-term exposure to PM_{2.5} major components and mortality in
445 the southeastern United States. *Environ Int* 158:106969.
- 446 9. Li Y, Henze DK, Jack D, Henderson BH, & Kinney PL (2016) Assessing public health

- burden associated with exposure to ambient black carbon in the United States. *Sci Total Environ* 539:515-525.
10. Cleland SE, Serre ML, Rappold AG, & West JJ (2021) Estimating the Acute Health Impacts of Fire-Originated PM(2.5) Exposure During the 2017 California Wildfires: Sensitivity to Choices of Inputs. *GeoHealth* 5(7):e2021GH000414-e002021GH000414.
 11. Reid CE, *et al.* (2016) Critical Review of Health Impacts of Wildfire Smoke Exposure. *Environ Health Persp* 124(9):1334-1343.
 12. Chen H, Samet JM, Bromberg PA, & Tong H (2021) Cardiovascular health impacts of wildfire smoke exposure. *Particle and Fibre Toxicology* 18(1):2.
 13. Lee SJ, *et al.* (2012) Comparison of Geostatistical Interpolation and Remote Sensing Techniques for Estimating Long-Term Exposure to Ambient PM2.5 Concentrations across the Continental United States. *Environ Health Persp* 120(12):1727-1732.
 14. Beckerman BS, *et al.* (2013) A Hybrid Approach to Estimating National Scale Spatiotemporal Variability of PM2.5 in the Contiguous United States. *Environmental Science & Technology* 47(13):7233-7241.
 15. Di Q, *et al.* (2016) Assessing PM2.5 Exposures with High Spatiotemporal Resolution across the Continental United States. *Environmental Science & Technology* 50(9):4712-4721.
 16. Hu XF, *et al.* (2017) Estimating PM2.5 Concentrations in the Conterminous United States Using the Random Forest Approach. *Environmental Science & Technology* 51(12):6936-6944.
 17. van Donkelaar A, Martin RV, Li C, & Burnett RT (2019) Regional Estimates of Chemical Composition of Fine Particulate Matter Using a Combined Geoscience-Statistical Method with Information from Satellites, Models, and Monitors. *Environmental Science & Technology* 53(5):2595-2611.
 18. Di Q, *et al.* (2019) An ensemble-based model of PM2.5 concentration across the contiguous United States with high spatiotemporal resolution. *Environ Int* 130.
 19. Park Y, *et al.* (2020) Estimating PM2.5 concentration of the conterminous United States via interpretable convolutional neural networks. *Environ Pollut* 256.
 20. Dennison PE, Brewer SC, Arnold JD, & Moritz MA (2014) Large wildfire trends in the western United States, 1984-2011. *Geophys Res Lett* 41(8):2928-2933.
 21. Radeloff VC, *et al.* (2018) Rapid growth of the US wildland-urban interface raises wildfire risk. *P Natl Acad Sci USA* 115(13):3314-3319.
 22. Zhang L, Lau W, Tao W, & Li Z (2020) Large Wildfires in the Western United States Exacerbated by Tropospheric Drying Linked to a Multi-Decadal Trend in the Expansion of the Hadley Circulation. *Environ Int* 140:e2020GL087911.
 23. Zou Y, Rasch PJ, Wang H, Xie Z, & Zhang R (2021) Increasing large wildfires over the western United States linked to diminishing sea ice in the Arctic. *Nat Commun* 12(1):6048.
 24. EPA (2012) EPAUS, Report to Congress on Black Carbon, <https://19january2017snapshot.epa.gov/www3/airquality/blackcarbon/2012report/fullreport.pdf>.
 25. McClure CD & Jaffe DA (2018) US particulate matter air quality improves except in wildfire-prone areas. *Proceedings of the National Academy of Sciences* 115(31):7901.
 26. Burnett R, *et al.* (2018) Global estimates of mortality associated with long-term exposure to outdoor fine particulate matter. *P Natl Acad Sci USA* 115(38):9592-9597.
 27. Collaborators GCD (2018) GBD 2017 Causes of Death Collaborators. Global, regional,

- 493 and national age-sex-specific mortality for 282 causes of death in;195 countries and
 494 territories, 1980-2017: a systematic analysis for the Global Burden of Disease Study 2017
 495 (vol 392, pg 1736, 2018). *Lancet* 392(10160):2170-2170.
- 496 28. Murray CJL, *et al.* (2020) Global burden of 87 risk factors in 204 countries and territories,
 497 1990-2019: a systematic analysis for the Global Burden of Disease Study 2019. *Lancet*
 498 396(10258):1223-1249.
- 499 29. Apte JS, Marshall JD, Cohen AJ, & Brauer M (2015) Addressing Global Mortality from
 500 Ambient PM_{2.5}. *Environmental Science & Technology* 49(13):8057-8066.
- 501 30. Wang TY, *et al.* (2019) Mortality burdens in California due to air pollution attributable to
 502 local and nonlocal emissions. *Environ Int* 133.
- 503 31. Aguilera R, Corringham T, Gershunov A, & Benmarhnia T (2021) Wildfire smoke impacts
 504 respiratory health more than fine particles from other sources: observational evidence from
 505 Southern California. *Nat Commun* 12(1).
- 506 32. Smith KR, *et al.* (2009) Public health benefits of strategies to reduce greenhouse-gas
 507 emissions: health implications of short-lived greenhouse pollutants. *Lancet*
 508 374(9707):2091-2103.
- 509 33. Rodriguez JD, Perez A, & Lozano JA (2010) Sensitivity Analysis of k-Fold Cross
 510 Validation in Prediction Error Estimation. *IEEE Transactions on Pattern Analysis and*
 511 *Machine Intelligence* 32(3):569-575.
- 512 34. Liang F, *et al.* (2020) The 17-y spatiotemporal trend of PM_{2.5} and its
 513 mortality burden in China. 117(41):25601-25608.
- 514 35. Chow JC, *et al.* (1993) The dri thermal/optical reflectance carbon analysis system:
 515 description, evaluation and applications in U.S. Air quality studies. *Atmospheric*
 516 *Environment. Part A. General Topics* 27(8):1185-1201.
- 517 36. Hitzenberger R, *et al.* (2004) Intercomparison of methods to measure the mass
 518 concentration of the atmospheric aerosol during INTERCOMP2000—influence of
 519 instrumentation and size cuts. *Atmos Environ* 38(38):6467-6476.
- 520 37. Li Z, *et al.* (2003) Evaluation of algorithms for fire detection and mapping across North
 521 America from satellite. 108(D2).
- 522 38. Pu R, *et al.* (2007) Development and analysis of a 12-year daily 1-km forest fire dataset
 523 across North America from NOAA/AVHRR data. *Remote Sens Environ* 108(2):198-208.
- 524 39. Buechi H, Weber P, Heard S, Cameron D, & Plantinga AJ (2021) Long-term trends in
 525 wildfire damages in California %J International Journal of Wildland Fire. 30(10):757-762.
- 526 40. Corona-Núñez RO, Li F, & Campo JE (2020) Fires Represent an Important Source of
 527 Carbon Emissions in Mexico. 34(12):e2020GB006815.
- 528 41. Rios B & Raga G (2019) Smoke emissions from agricultural fires in Mexico and Central
 529 America. 13 %J Journal of Applied Remote Sensing(3):036509.
- 530 42. Hammer MS, *et al.* (2020) Global Estimates and Long-Term Trends of Fine Particulate
 531 Matter Concentrations (1998–2018). *Environmental Science & Technology* 54(13):7879-
 532 7890.
- 533 43. Prichard SJ, *et al.* (2020) Wildland fire emission factors in North America: synthesis of
 534 existing data, measurement needs and management applications. *International Journal of*
 535 *Wildland Fire* 29(2):132-147.
- 536 44. Zhang X, Hecobian A, Zheng M, Frank NH, & Weber RJ (2010) Biomass burning impact
 537 on PM_{2.5} over the southeastern US during 2007: integrating chemically
 538 speciated FRM filter measurements, MODIS fire counts and PMF analysis. *Atmos. Chem.*

- 539 *Phys.* 10(14):6839-6853.
- 540 45. Hand JL, Schichtel BA, Pitchford M, Malm WC, & Frank NH (2012) Seasonal
541 composition of remote and urban fine particulate matter in the United States. *J Geophys*
542 *Res-Atmos* 117.
- 543 46. Hand JL, Prenni AJ, Copeland S, Schichtel BA, & Malm WC (2020) Thirty years of the
544 Clean Air Act Amendments: Impacts on haze in remote regions of the United States (1990-
545 2018). *Atmos Environ* 243.
- 546 47. Jiang Z, *et al.* (2018) Unexpected slowdown of US pollutant emission reduction in the past
547 decade. *P Natl Acad Sci USA* 115(20):5099-5104.
- 548 48. Luben TJ, *et al.* (2017) A systematic review of cardiovascular emergency department visits,
549 hospital admissions and mortality associated with ambient black carbon. *Environ Int*
550 107:154-162.
- 551 49. Ford B, *et al.* (2018) Future Fire Impacts on Smoke Concentrations, Visibility, and Health
552 in the Contiguous United States. 2(8):229-247.
- 553 50. Watson JG, Chow JC, Moosmueller H, Green M, & Frank N (1998) Guidance for using
554 continuous monitors in PM_{2.5} monitoring networks. (United States), p Medium: P; Size:
555 188 p.
- 556 51. Solomon PA, *et al.* (2014) U.S. National PM_{2.5} Chemical Speciation Monitoring
557 Networks—CSN and IMPROVE: Description of networks. *Journal of the Air & Waste*
558 *Management Association* 64(12):1410-1438.
- 559 52. Lyapustin A, Wang YJ, Korkin S, & Huang D (2018) MODIS Collection 6 MAIAC
560 algorithm. *Atmos Meas Tech* 11(10):5741-5765.
- 561 53. Garay MJ, *et al.* (2020) Introducing the 4.4 km spatial resolution Multi-Angle
562 Imaging SpectroRadiometer (MISR) aerosol product. *Atmos. Meas. Tech.* 13(2):593-628.
- 563 54. Gelaro R, *et al.* (2017) The Modern-Era Retrospective Analysis for Research and
564 Applications, Version 2 (MERRA-2) %J Journal of Climate. 30(14):5419-5454.
- 565 55. Crippa M, *et al.* (2018) Gridded emissions of air pollutants for the period 1970–2012 within
566 EDGAR v4.3.2. *Earth Syst. Sci. Data* 10(4):1987-2013.
- 567 56. Ichoku C & Ellison L (2014) Global top-down smoke-aerosol emissions estimation using
568 satellite fire radiative power measurements. *Atmos Chem Phys* 14(13):6643-6667.
- 569 57. Hersbach H, *et al.* (2020) The ERA5 global reanalysis. 146(730):1999-2049.
- 570 58. Muñoz-Sabater J, *et al.* (2021) ERA5-Land: a state-of-the-art global reanalysis dataset for
571 land applications. *Earth Syst. Sci. Data* 13(9):4349-4383.
- 572 59. Farr TG, *et al.* (2007) The Shuttle Radar Topography Mission. 45(2).
- 573 60. Didan K (2021) MODIS/Terra Vegetation Indices Monthly L3 Global 1km SIN Grid V061
574 [Data set]. *NASA EOSDIS Land Processes DAAC*.
- 575 61. Bright EA, Coleman PR, Dobson JE, & Sensing R (2000) LandScan: A Global
576 Population Database for Estimating Populations at Risk. 66:849-858.
- 577 62. Wei J, *et al.* (2019) Estimating 1-km-resolution PM_{2.5} concentrations across China using
578 the space-time random forest approach. *Remote Sens Environ* 231.
- 579 63. Gueymard CA & Yang D (2020) Worldwide validation of CAMS and MERRA-2 reanalysis
580 aerosol optical depth products using 15 years of AERONET observations. *Atmos Environ*
581 225:117216.
- 582 64. Shi H, Xiao Z, Zhan X, Ma H, & Tian X (2019) Evaluation of MODIS and two reanalysis
583 aerosol optical depth products over AERONET sites. *Atmospheric Research* 220:75-80.
- 584 65. Zhou Z-H & Feng J (2017) Deep forest: towards an alternative to deep neural networks. in

585 *Proceedings of the 26th International Joint Conference on Artificial Intelligence (AAAI*
586 *Press, Melbourne, Australia), pp 3553–3559.*
587